Article type : Original Article

Color : Figs 1-3, 6 & 8

Title page

Title: Visualization of the activation of the histamine H3 receptor (H3R) using novel Fluorescence Resonance Energy Transfer Biosensors and their potential application to the study of H3R pharmacology

The names and affiliations of the authors are as follows:

Ying Liu, Hong Zeng, John D. Pediani, Richard J. Ward, Lu-Yao Chen, Nan Wu, Li Ma, Mei Tang, Yang Yang, Su An, Xiao-Xi Guo, Qian Hao, Tian-Rui Xu*

Tian-Rui Xu (☒)

Ying Liu, Hong Zeng, Lu-Yao Chen, Nan Wu, Li Ma, Mei Tang, Yang Yang, Su An, Xiao-Xi Guo, Qian Hao, Tian-Rui Xu.

Faculty of Life Science and Technology, Kunming University of Science and Technology, Kunming, Yunnan, China 650500

This article has been accepted for publication and undergone full peer review but has not been through the copyediting, typesetting, pagination and proofreading process, which may lead to differences between this version and the Version of Record. Please cite this article as doi: 10.1111/febs.14484

John D. Pediani, Richard J. Ward.

Molecular Pharmacology Group, Institute of Molecular, Cell and Systems Biology, College of Medical, Veterinary and Life Sciences, University of Glasgow, Glasgow G12 8QQ, Scotland, United Kingdom

Corresponding author:

Tian-Rui Xu

Faculty of Life Science and Technology

Kunming University of Science and Technology, Kunming, Yunnan, China 650500

Email: tianruixu@kmust.edu.cn

Tel.: + 86 87165933100

Running Title: Visualization of the activation of the H3R by FRET

Abbreviation: H3R: Histamine-3 receptor; FRET: Fluorescence Resonance Energy Transfer; CFP: cyan fluorescent protein; YFP: yellow fluorescent protein; GPCRs: G protein-coupled receptors; Ach: acetyl choline; AD: Alzheimer's disease; PLA2: phospholipase A2; MAPK: mitogen-activated protein kinase; DMEM: Dulbecco's Modified Eagle's medium; PVDF: polyvinylidene difluoride; VSV-G: vesicular stomatitis virus G; mGluR5: the metabotropic glutamate 5 receptor; CLO: clobenpropit; IME: imetit; p-ERK: phosphorylated ERK; Flp-in: Flp-In^{TM} T-REx^{TM} 293 cells.

Key words: Histamine-3 receptor, Biosensor, FRET, Kinetic characters, Drug

Conflict of interest statement

The authors declare no conflicts of interest.

Ying Liu[1], Hong Zeng[1], John D. Pediani[2], Richard J. Ward[2], Lu-Yao Chen[1], Nan Wu[1], Li Ma[1], Mei Tang[1], Yang Yang[1], Su An[1], Xiao-Xi Guo[1], Qian Hao[1], Tian-Rui Xu[1*]

[1]Faculty of Life Science and Technology, Kunming University of Science and Technology, Kunming, Yunnan, China 650500

[2] Molecular Pharmacology Group, Institute of Molecular, Cell and Systems Biology, College of Medical, Veterinary and Life Sciences, University of Glasgow, Glasgow G12 8QQ, Scotland, United Kingdom

Abstract

Activation of the Histamine-3 receptor (H3R) is involved in memory processes and cognitive action, whilst blocking H3R activation can slow the progression of neurological disorders such as Alzheimer's disease, schizophrenia and narcolepsy. To date however no direct way to examine the activation of H3R has been utilised. Here, we describe a novel biosensor which can visualise the activation of H3R through an intramolecular Fluorescence Resonance Energy Transfer (FRET) signal. To achieve this, we constructed an intramolecular H3R FRET sensor with cyan fluorescent protein (CFP) attached at the C-terminus and yellow fluorescent protein (YFP) inserted into the third intracellular loop. The

sensor was found to internalize normally on agonist treatment. We measured FRET signals between the donor CFP and the acceptor YFP in living cells in real time, the results of which indicated that H3R agonist treatment (imetit or histamine) increases the FRET signal in a time- and concentration-dependent manner with Kon and Koff values consistent with published data and which maybe correlated with decreasing cAMP levels and the promotion of ERK1/2 phosphorylation. The FRET signal was inhibited by H3R antagonists and the introduction of mutations at F419A, F423A, L426A and L427A, once again, the promotion of ERK1/2 phosphorylation was diminished. Thus, we have built a H3R biosensor which can visualise the activation of receptor through real time structure changes and which can obtain pharmacological kinetic data at the same time. The FRET signals may allow the sensor to become a useful tool for screening compounds and optimising useful ligands.

Introduction

Histamine, a neurotransmitter, is involved in multiple physiological processes by coupling to four distinct, but related, G protein-coupled receptors (GPCRs): H1Rs, H2Rs, H3Rs, and H4Rs [1-3]. The involvement of histamine receptors (HRs) in the cognitive process has long been confirmed, especially in the case of H3Rs [2, 4]. The H3R is mainly expressed in nerve terminals, where it participates in the processes of memory and cognitive action [5]. There is also increasing evidence that blockade of central nervous system H3Rs could enhance the cortical fast rhythms closely associated with cognitive behavior [6] and indeed, several drug candidates that block the H3R have been shown to increase the release of acetyl choline (ACh), and therefore alleviate symptoms and slow the progression of Alzheimer's disease (AD) in clinical trials [7-9]. Thus far, the most recent success is the pitolisant, which showed protective effects against human narcolepsy and has entered phase III of clinical development [10]. Activation of Gi/o proteins by H3 receptors results in two main intracellular actions, the reduction of cAMP formation [11] and the inhibition of voltage-activated calcium channels, which leads to a decrease in intracellular Ca^{2+} levels by impairing the entrance of Ca^{2+} through voltage-gated ion channels [5, 12, 13]. In addition, Gi/o activation via H3 receptors can activate PI3K, leading to the subsequent activation and phosphorylation of Akt [11]. The activation of

H3Rs also results in the activation of mitogen-activated protein kinase (MAPK) pathways, especially ERK1/2 phosphorylation [14, 15].

A number of methods are available for studying GPCR activation including the cAMP assay [16], Ca^{2+} release assay [17], ERK1/2 phosphorylation assay [18] and the β-arrestin recruitment assay [19, 20], however whilst each of these methods is able to detect GPCR activation, they do so only indirectly. Recently however FRET based probes/ biosensors have been developed that avoid this deficiency in more traditional techniques.

The first report of a novel sensor class, built on the basis of a GPCR was published in 2003 and served as a proof of principle for the use of FRET biosensors in living cells [21]. Although the development of such FRET sensors proceeded slowly, they have made their way into the standard toolbox for GPCR research as several groups are now reporting on the generation and use of these sensors. By now, FRET sensors have been reported for a significant portion of GPCRs, such as the α2-, β2-adrenoceptors [22, 23], M1-, M2-, M3-, M5-muscarinic cholinergic receptors [23-26], A2A-adenosine receptor [22, 27], 5-HT_{1B} receptor [28] and the orexin-1 and -2 receptors [29]. No doubt this list will continue to grow. In recent studies these sensors have been used to investigate receptor dynamics in living cells to evaluate ligand binding and ligand efficacy in real time, to study voltage and mechano-sensitivity of GPCRs or to study the influence of receptor polymorphisms on receptor function in real-time [30].

There are two basic types of such FRET reporter systems and these are known as intermolecular and intramolecular sensors. Intermolecular FRET sensors are established tools that measure increases in the FRET ratio that is generated by, for instance, a suitably labelled species translocating from cytosol to membrane to interact with a suitably labelled membrane localized species, for example in the β-arrestin recruitment assay. FRET-based intramolecular sensors (both FRET donor and acceptor are part of the same species) are well established and useful tools to, for instance,

detect changes in small molecule concentrations at subcellular resolution [31-33]. By the use of intramolecular FRET however, we can measure ligand-induced GPCR activation. The basis of the technique is that ligand binding induces small conformational changes within the GPCR around the ligand binding site, which are then amplified to become larger movements at the cytoplasmic face of the receptor, in turn transmitting a signal to a G protein [34, 35]. Thus, if a FRET donor and acceptor are fused at appropriate locations within the GPCR polypeptide their relative distance or orientation may change leading to a modification of the FRET signal. The FRET signal of GPCR FRET sensor described in this paper is designed to estimate the forces and their distribution in time and space in live cells and to probe the transfer of energy from a donor, such as CFP, to an acceptor, such as YFP, followed with ligand binding and resulting in signal propagation across the cell membrane [31-33, 36].

Herein, we describe a FRET biosensor which is able to quantitate H3R activation directly. It was used to monitor concentration- and time-dependent effects of receptor activation by agonists in real time. Analysis of receptor kinetics induced by ligands supported the view that receptor modulation occurs in a very rapid manner. The FRET sensor developed and used in this study can be used to examine ligand binding kinetics, study the details of receptor activation mechanisms and otherwise explore the activation of receptors in living cells.

Results

Design of the Potential Intramolecular H3 Receptor FRET Sensors

In this study, a biosensor derivative of the histamine H3 receptor was constructed by fusing CFP in frame to the C-terminal tail of the full-length human H3 receptor. The vesicular stomatitis virus G, (VSV-G) peptide, epitope was also inserted in the extracellular N-terminal domain together with an N-terminal leader sequence from the metabotropic glutamate receptor 5 (Figure 1A). Based on our previous report [29], we inserted YFP into the third intracellular loop, replacing all but the 12 amino acids from each end of the loop which were retained (Figure 1A). Thus, 118 amino acids of the third

intracellular loop of the H3 receptor (from position 230 to position 347) were replaced by YFP sequence (Figure 1B), resulting in the plasmid mGluR5-VSV-G-H3-YFP-CFP (Figure 1A). This plasmid was transiently transfected into HEK293 cells and fluorescence measurements were taken. Results showed that the sensor was expressed, but mainly located in the cytosol, not at the cell membrane (Figure 1C). Subsequently, stable cell lines were constructed by transfecting the mGluR5-VSV-G-H3-YFP-CFP plasmid into Flp-In™ T-REx™ 293 cells. These cells allow inducible and regulated expression of constructs cloned into the Flp-In™ locus [37]. In these cells, induction of construct expression in the presence of doxycycline resulted in clear membrane localization of the receptor sensor (Figure 1D). The cells that expressed mGluR5-VSV-G-H3R-YFP-CFP were selected and used for further studies.

Functional characterization of the intramolecular H3 receptor FRET sensor

Classically, agonist-induced GPCR activation results in the activation of heterotrimeric G proteins. Upon continuous agonist stimulation, GPCR activation diminishes through a process known as desensitization [38]. GPCR internalization has long been considered to play a major role in the desensitization process, it is also involved in receptor re-sensitization and the ligand scavenging function of some atypical receptors. Thus, internalization contributes to the diversity of GPCR-dependent signaling [39], and its dynamics and quantification in living cells has generated considerable interest [40, 41]. In the case of the H3R some evidence has suggested that this receptor also experiences homologous desensitization in response to agonist exposure [42]. To visualise the movement of the receptor from cell surface to punctate intracellular vesicles, CFP was imaged in cells induced to express mGluR5-VSV-G-H3R-YFP-CFP using fluorescence microscopy. Upon treatment with the agonist imetit, (10^{-6} M), the localization of CFP gradually moved from the cell surface to the cell interior in a time-dependent manner (Figure 1E). Cell surface biotinylation studies were performed to measure the potency of imetit to cause this effect. Cells induced to express mGluR5-VSV-G-H3R-YFP-CFP were treated either with 10^{-6} M imetit for up to 60 min or with varying doses of imetit for 40 min. Subsequently, the cells surface proteins were labeled with biotin that was then captured by streptavidin linked beads and analysed by SDS-PAGE and western blotting using an

anti-VSV-G antibody to detect the FRET sensor. Results showed the presence of a single polypeptide (95 kDa) in the absence of imetit (Figure 1 F and G). However, with increasing time and dose of imetit, the level of biotinylated polypeptide detected with anti-VSV-G was reduced (Figure 1 F and G). This is consistent with the H3R FRET sensor internalizing upon agonist treatment in a similar way to the wild type H3R [43].

Detection of FRET by photo-bleaching acceptors

The pooled acquired prebleach donor and acceptor image sequences indicated that our attenuated illumination experimental laser set up evoked some negligible bleaching, as we consistently found a reduction in CFP and YFP fluorescent intensity from one time point to the next (see traces Figure 2G). It was also observed that the acceptor YFP faded slightly faster (Figure 2A-B and 2E-F) than the donor CFP (Figure 2C-D and 2E-F), and this could be due to the 440 nm laser line having an added excitation effect upon the acceptor. High intensity laser illumination photobleaching destruction of the acceptor (YFP) indicated that the donor was converted from a quenched state to an unquenched state as a concomitant increase in donor fluorescence intensity was observed in the acquired post-bleach set of donor images (Figure 2G, see donor trace). This result suggested that our set up was sensitive enough to detect FRET. The evaluated FRET efficiency was quantified to be 15.8%.

(FI = 2400 / FI = 2850; 2400/2850 = 0.842; 1 – 0.842 = 0.158; 0.158 times 100 = 15.8%)

Agonist-induced inhibition of cAMP activity is concentration-dependent

According to conventional models of GPCR activation, when an agonist is used to stimulate a GPCR then downstream signaling events can be monitored. To this end we measured cAMP levels as an indicator of H3 receptor activation. As shown in Figure 1H, the H3 agonists' histamine and imetit potently inhibited the 10 μM forskolin-stimulated production of cAMP in a concentration-dependent manner in H3 receptor sensor expressing cells. Half maximal inhibitory concentration (IC50) of imetit were produced with 0.4744 ± 0.0742 pM, the maximum or minimum was 106.80 ± 2.00 or 17.78

± 1.47. Moreover, IC50 of histamine were produced with 0.6927 ± 0.0531 pM, the maximum or minimum was 110.90 ± 1.39 or 24.14 ± 1.07.

Agonist-induced activation of Intramolecular H3 Receptor FRET Sensors

To determine whether orthosteric activation of H3R by histamine or imetit was sufficient to activate the probe, sensors were analysed for their ability to produce an agonist modifiable FRET signal. Activation by full agonist (histamine or imetit) brought CFP and YFP fluorophores into either closer proximity or a more favorable (to the generation of a FRET signal) orientation, or both, thereby increasing FRET. The FRET signals of the intracellular sensors were recorded by measuring changes in FRET efficiency in the stably transfected cell line. Treatment with histamine (Figure 3A) or imetit (Figure 3B) increased the FRET signals in cells induced to express mGluR5-VSV-G-H3R-YFP-CFP, in a time- and dose-dependent manner. Study of the kinetics of sensor response showed that the kinetic curve was changed with histamine or imetit administration. Half-maximal effects of histamine were produced with 6.65 ± 0.11 nM (Fig. 3C), while imetit was less potent (EC50=9.15 ± 0.14 nM) (means ± S.E., *n* = 5).

To determine the kinetic characters of the receptor, we calculated the association rate constant (Kon) and the dissociation rate constant (Koff). Then the dissociation constant (Kd) was calculated on the basis of the definition of the affinity constant (Kd = Koff / Kon), from this one can estimate the changes in the association energy. The studies indicated that the sensor construct bound to histamine with nanomolar affinity (10^{-5} M histamine, Kd = 3.60 ± 0.06 nM; 10^{-6} M, Kd = 3.53 ± 0.05 nM; 10^{-7} M, Kd = 3.87 ± 0.11 nM; 10^{-8} M, Kd = 3.73 ± 0.04 nM; 10^{-9} M, Kd = 3.72 ± 0.06 nM, means ± S.E., *n* = 5) (Table.1). This is similar to the published Kd values for histamine [44-46]. Furthermore, imetit with the H3 receptor sensor affinity was also calculated with nanomolar affinity (10^{-5} M imetit, Kd = 4.72 ± 0.06 nM; 10^{-6} M, Kd = 4.81 ± 0.07 nM; 10^{-7} M, Kd = 4.75 ± 0.03 nM;

10^{-8} M, Kd = 4.75 ± 0.01 nM; 10^{-9} M, Kd = 4.57 ± 0.06 nM, means ± S.E., *n* = 5) (Table.1). This is also similar to the published Kd values for histamine [47, 48]. The results demonstrate therefore that this is a very fast association [46, 49, 50] and that both histamine and imetit showed the expected behavior, in that they were able to increase the nFRET signal in a time and concentration dependent manner. Analysis of kinetics of receptors induced by different agonists in living cells showed that receptor modulation occurs very rapidly, and different agonists act differently on different receptor subtypes [51].

To determine whether ERK phosphorylation can be correlated with the changes in the FRET curve, the level of ERK phosphorylation was evaluated by western blot analysis. As shown in Figures 3D and F, the expression of mGluR5-VSV-G-H3R-YFP-CFP was strongly induced after treatment with doxycycline, and its expression was found to be agonist independent in the cells that show inducible and regulated expression of constructs cloned into the Flp-In™ T-REx™ 293 cells locus [37]. Furthermore, histamine or imetit treatment significantly increased phosphorylated ERK in a dose-dependent manner (Figures 3E and G). These results indicate that agonist treatment of mGluR5-VSV-G-H3R-YFP-CFP expressing cells was able to activate the ERK signaling pathway.

Characterization of H3 receptor FRET sensor expression by radioligand binding

Cells induced to express the mGluR5-VSV-G-H3R-YFP-CFP construct were used in intact cell ligand binding studies using [^{3}H]-histamine, an agonist of H3 receptor [52-54]. These studies also indicated that the sensor construct bound this ligand with nanomolar affinity (Kd = 6.82 ± 0.18 nM, mean ± S.E., *n* = 3) (Fig. 4). This demonstrated similar binding affinity to that obtained from FRET method.

[^{3}H]-histamine competition binding

The accuracy of rate constants calculated for unlabeled compounds is highly dependent upon the precision of the kinetic parameters defined for the radioligand. Initial experiments were therefore performed to fully characterize the kinetic parameters of [^{3}H]-histamine. 10 nM [^{3}H]-histamine was used to experimentally determine the Koff value. And 10 μg well^{-1} cells membranes were used in the experiment. [^{3}H]-histamine dissociation was found to be monophasic and gave a half-time of dissociation ($t_{1/2}$) of 12.08 ± 2.26 min (n = 3) (Figure 5A) which when applied to Equation 1 gave a Koff of 0.057 ± 0.0003 min^{-1} (n = 3).

Since the association rate of a ligand is, in part, dependent upon the concentration used, we constructed a series of kinetic association curves using a range of [^{3}H]-histamine concentrations. Each association curve was monitored until equilibrium for that concentration ($Y_{max)}$ was reached (Figure 5B). Using the value for Koff described above, the mean Kon value was calculated as 8.16 ± 0.19×10^4 M^{-1} min^{-1}. Furthermore, the kinetically derived Kd (Koff/Kon) calculated from the mean values for individual experiments (7.00 ± 0.24 nM) is in good agreement which the value obtained from [^{3}H]-histamine saturation binding experiments (6.82 nM). Furthermore, this result is in good agreement with values obtained by Esbenshade TA *et al* [55]. This result is also consistent with the Kd value obtained from FRET method.

The H3R sensors report conformational changes in response to antagonist application

We used clobenpropit, an antagonist of H3R, to treat the cells and as anticipated, the addition of this antagonist at 10^{-6}M resulted in a blocking effect upon the activation by imetit (Figure 6). However, removal of imetit and potential wash-out of imetit did not result in a rapid reversal of the FRET changes (Figure 6). This is consistent with sustained residency of the agonist on the receptor.

The H3R-mediated phosphorylation of ERK1/2 signaling pathways is inhibited by ciproxifan and clobenpropit

ERK1/2 pathway is a critical effector of downstream GPCR signaling. Western blotting analysis was performed to determine whether ERK1/2 signaling pathway was activated by agonist treatment of mGluR5-VSV-G-H3R-YFP-CFP expressing cells. As shown in Figure 7A-D, treatment with histamine or imetit significantly increased phosphorylation of ERK1/2 in a time-dependent manner. However, this increase was significantly attenuated by ciproxifan or clobenpropit pretreatment. This suggests that binding of agonists to H3 receptor intramolecular sensor promoted the activation of downstream signaling pathways and the H3 receptor intramolecular sensors have biological activity. The results of ERK phosphorylation were also consistent with changes of FRET baselines. Constitutive activity of Gi-coupled GPCRs can be assessed by measuring inverse agonist-induced reduction of mitogen-activated protein kinase (MAPK) activity [56]. In the present study, western blotting analysis was performed to determine whether ERK1/2 phosphorylation was inhibited by pretreatment with the inverse agonist ABT-293. As unexpected, the results demonstrated that a histamine- or imetit-induced increase in ERK1/2 phosphorylation was inhibited by ABT-239 application (Fig. 7E-F). Therefore, the results indicated that at least for the ERK1/2 signalling pathway, the H3R biosensor lacks constitutive activity.

Mutation of Phe-419, Phe-423, Leu-426 and Leu-427 in H3 Greatly Reduces Potency of imetit

To further explore the activation of the FRET sensor determine we introduced a number of mutations into the H3R, following which changes in FRET at baseline and also the phosphorylation of ERK were evaluated. Previous studies have shown that Phe-419, Phe-423, Leu-426, and Leu-427 are important for coupling of the H3Rs to their cognate G proteins, and these amino acids are located at helix 8 in the carboxy-terminal tail of the human H3 receptor [57]. In the present study, these hydrophobic aromatic and aliphatic amino acids were changed to Ala (hydrophobic, but small) in the mGluR5-VSV-G-H3R-YFP-CFP sensor, and Flp-In^{TM} T-REx^{TM} 293 cell lines that express the mutated constructs, in the presence of doxycycline, were produced. Treatment of these mutant FRET sensor cell lines with the agonist imetit showed a loss of agonist activity, indeed, this form of the FRET

sensor failed to respond to the administration of imetit (Figure 8A). The introduction of these mutations, however, had no effect upon the expression level of the sensor as measured by α-VSV-G immunoblotting (Figure 8B). Compared to the non-mutated H3 receptor intramolecular sensor, at which the highest concentration of imetit (1×10^{-6} M) caused significant increases in phosphorylation of ERK1/2 as shown by western blotting analysis (Figure 8C), the point mutation of F419A, F423A, L426A, and L427A resulted in similar levels of decrease in ERK1/2 phosphorylation.

This decreased ERK1/2 phosphorylation induced by the various point mutations correlated with the attenuation of FRET signals (Figure 8A and C). The results suggest that the loss of agonist activation mutations in the H3 receptor disrupt function of the intramolecular sensor and activation of downstream signaling pathways. Furthermore, results showed that the FRET sensors technique and phosphorylation of ERK method are in agreement.

Discussion

H3 receptor has been described as a key mediator in many diseases and is recognized as a potential target for treatment of cardiovascular disorders, inflammatory conditions, Alzheimer's disease and attention deficit hyperactivity disorder [58]. Moreover, blockade of the neuronal H3 receptor was also demonstrated to have neuroprotective effects in *in vitro* ischemia models [7]. These observations highlight the importance of screening and characterizing inverse agonist and hence neuroprotective ligands at the H3 receptor. However, there are, at present, few quick and effective tools for achieving this goal. Herein we describe the construction of FRET sensors based upon the Gi-coupled histamine-3 receptor as a direct detection tool to investigate receptor activation. Compared with other indirect methods, such as the cAMP production assay, the Ca^{2+} release assay, the ERK1/2 phosphorylation assay and the β–arrestin recruitment assay, the FRET sensor signal from receptor activation was not affected by other factors, such as downstream signals, the solubility of ligands. The H3R sensor exhibited a strong and rapid increase in the FRET signal when stimulated with the agonists histamine or imetit (Figures. 3 to 8). This is consistent with the results described for the Gi-coupled 5-HT-1B FRET sensor when stimulated with 5-hydroxytryptamine (5-HT) [28]. This is a clear contrast with the Gq-coupled orexin-1 receptor FRET sensor and orexin-2 receptor FRET

sensor, which showed a slow decrease in the FRET signal when stimulated with agonists [29]. Whilst, the similarly Gq-coupled to muscarinic M1, M3 and M5 acetylcholine receptor sensors showed a maximal increase in the FRET signal upon agonist exposure [59]. This difference might be explained by the different agonist classes (small molecule as opposed to peptide) mediating GPCR activation or possibly the different orientation factors between the two fluorophores rather than alternative movements of the helices upon receptor activation. Therefore, the reports strengthen the notion of a possible influence of orientation factors in the observed change of the FRET signals.

Since the FRET-based approach represents a unique tool to monitor changes in receptor conformation in real time, we analysed the kinetics of the different orthosteric ligands used in this study. The basis of monitoring ligand-induced GPCR activation by intramolecular FRET is that ligand binding induces small conformational changes within the GPCR around the ligand binding site, which are then amplified to become larger movements at the cytoplasmic face of the receptor, in turn transmitting a signal to (usually, but not always) a G protein. Receptor activation for the H3R sensors occurred rapidly at histamine and imetit exposure in a concentration and time dependent manner (Fig. 3). Then we used the FRET sensors to study the dynamics of the interaction between ligands and GPCRs in live cells and calculated kinetic parameters, Kon and Koff of ligand binding for the first time (Table. 1). Next, we calculated the affinity constant (Kd). These data are in good agreement with the published binding affinities of H3R agonist ligands for stimulation with the endogenous or exogenous receptor agonists [60].

From previous studies we know that downstream ERK1/2 phosphorylation is a good and widely used indicator of GPCR activation [15]. The importance of ERK1/2 phosphorylation in the process of neuronal survival and memory has been demonstrated many times [61]. Indeed, neuroprotective effects associated with activation of ERK phosphorylation may attenuate the extent of neuron injury in various animal models [62]. Consistent with this observation, the H3R activation here induced similar changes in ERK1/2 phosphorylation (Fig. 3 to 8) and has previously been described as full agonists for the decrease of cAMP production (Fig. 1H). We found that agonist of H3 receptor such

as histamine, imetit, methythistamine and dimaprint could promote ERK activation and present association with neuron protection. The study further demonstrated that activation of the ERK pathway is an important signaling conduit following H3R activation. The kinetics of FRET signal change with cAMP inhibition and ERK1/2 phosphorylation are consistent, which strongly suggest that FRET signal change is the direct indicator of GPCR activation.

The importance of the identification and analysis of novel (and pharmacologically useful) GPCR ligands, together with the further analysis of those which are already known cannot be overstated. A number of GPCRs have recently emerged as potential drugs targets, even though their endogenous ligands maybe as yet unknown [63]. The fluorescence based techniques described here may well be applicable to the study of the interactions between ligands and these "orphan" GPCRs [64, 65]. Other forms of FRET sensors may additionally serve as important tools for studying the dynamic changes in the intracellular level of signaling molecules and metabolites in living cells. The aim of this study was to experimentally test the widespread of using of donor-acceptor FRET transfer rates to predict the ensemble FRET efficiency [66-69].

FRET biosensors such as that described here may prove to be adaptable for ligand library screening, investigation of the kinetics of ligand binding and a host of other pharmacological analyses. There are FRET sensors available that can enable screens for a variety of important targets in their native cellular environment, screens that cannot be conducted in any other way than with FRET sensors, such as biased drugs, inverse agonists and antagonists.

In conclusion, the H3 receptor sensors described in the present study reveal novel insights into H3 receptor activation and it has been shown that the observed agonist activation dynamics are consistent with published pharmacological characteristics of H3 receptor. Therefore, the receptor sensors may provide a method to detect and even visualise H3 receptor activation in real time with high kinetic resolution, which could not be fulfilled by other biochemical techniques and may help to further screen drugs for H3 receptor modulation.

Materials and Methods

Materials

Doxycycline, imetit dihydrobromide, clobenprapit dihydrobromide, methylhistamine, dimaprint, ciproxifan, ABT-239, and monoclonal mouse anti-VSV-G antibodies were obtained from Sigma-Aldrich (Gillingham, UK). [^{3}H]-histamine (specific activity 1 mCi mmol^{-1}) was obtained from Amersham Biosciences U.K. Ltd (GE Healthcare, Chalfont St Giles, UK). Lipofectamine 2000 transfection reagent was purchased from Invitrogen (Gibco, Germany). Protease inhibitor cocktail tablets were purchased from Millipore (Merck Millipore, Germany). Monoclonal rabbit p44/42 mitogen-activated protein kinase (MAPK; ERK1/2) and polyclonal rabbit phospho-p44/42 MAPK (phosphor-ERK1/2) antibodies were obtained from Cell Signaling Technology (Cell Signaling Technology, USA). All other reagents were obtained from Thermo Fisher Scientific (Waltham, MA, USA) and Sigma Aldrich (Gillingham, UK).

Construction of the H3R FRET-sensors

Intramolecular FRET sensors of the human H3R comprised a C-terminally fused enhanced CFP, which acted as energy donor and an enhanced YFP, which acted as energy acceptor, inserted into the 3rd intracellular loop. The construct was generated by, firstly, replacing the Orexin-1 receptor sequence of pcDNA5/FRT/TO- VSV-G-h-Orexin-CFP [29] with histamine-3 receptor sequence by using the In-Fusion HD Cloning Kit (Clontech) to make pcDNA5/FRT/TO-VSV-G-histamine -3-CFP. A linearized vector was generated by PCR using the following primers: sense, 5'-ATGGTGAGCAAGGGCGAGG-3'; antisense primer, 5'-CTTACCAAGGCGGTTCATTTCG-3'. Subsequently, histamine 3-specific primers with 15 bp extensions homologous to vector ends were designed. The sequences of these primers were sense 5'-AACCGCCTTGGTAAGATGGAGCGCGCGCCGCCCGA-3'; antisense primer, 5'-CTTCCAGCAGTGCTCCAGGGCCTCGGCAGACGTGT-3'. Subsequently, YFP was inserted into the third intracellular loop of the histamine-3 receptor; 12 amino acids were retained at each end of the loop. The primers used were sense 5'-ATCCAGAGGCGCACCAT

GGTGAGCAAGGGCGAGGAGCTGTTC-3′; antisense primer, 5′-CGACTTGGCCACTTTC

TTGTACAGCTCGTCCATGCCGAGAG-3′.

Generation and maintenance of H3R stable Flp-In™ T-REx™ 293 cells

To generate Flp-In™ T-REx™ 293 cells capable of expressing the FRET sensor constructs on induction, cells were transfected with a mixture containing the desired protein cDNA subcloned into the pcDNA5/FRT/TO vector and the pOG44 plasmid at a 1:9 ratio. Transfection was performed using Lipofectamine 2000 transfection reagent (Invitrogen) according to the manufacturer's instructions. After 48 h, the medium was supplemented with 200 μg/ml hygromycin B to select for stably transfected cells. Cells were treated with 1μg/ml doxycycline for 24 h to induce the expression of desired protein, followed by screening for fluorescence corresponding to CFP and for VSV-G protein expression by western blotting.

HEK 293T cell culture and transfection

HEK 293T cells were maintained in Dulbecco's Modified Eagle's medium (DMEM) supplemented with 0.292 g/L L-glutamine, 1% antibiotic mixture, and 10% (v/v) newborn calf serum at 37°C in a 5% CO_2 humidified atmosphere. For transient expression the cells were transfected with FRET sensor constructs using Lipofectamine 2000 transfection reagent (Invitrogen) according to the manufacture's protocols. Twenty-four hours after transfection, cells were screened for fluorescence corresponding to CFP and YFP.

Cyclic AMP assay

The stably transfected cells were plated into 96-well plates (typically between 6-10$\times 10^3$ cells/well) 24 hrs prior to assay and simultaneously induced with 100 ng/ml doxycycline. Thereafter, the cells were incubated for exactly 10 min with fresh medium supplemented with 10 μM forskolin, and then

treated with different concentrations (10^{-5} M, 10^{-6} M, 10^{-7}M, 10^{-8} M, 10^{-9} M and 0 M) of histamine or imetit for 5 minutes. After treatment, the cells were rinsed twice with 200 µl cold PBS, and 100 µl/well 1× cell lysis buffer (#9803, cell signaling technology) added and the cells incubated on ice for 5 to 10 minutes. cAMP assays were then carried out using an ELISA kit, following the manufacturer's instructions (Cell Signaling Technology). The amount of cAMP in each sample was calculated from a cAMP standard curve (0, 80, 26.7, 8.9, 3.0, 1.0 and 0.3 pmol/ml), using the non-linear regression-fitting function of the software package Prism 5.0. The percentage of activity is calculated as follows: % level = $100 \times [(A\text{-}A_{basal}) / (A_{max}\text{-}A_{basal})]$, where A is the sample absorbance, A_{max} is the absorbance at maximum stimulation (high histamine or imetit concentration) and A_{basal} is the absorbance at basal level (no histamine or imetit).

Western Blotting assay

Cells samples were washed once in cold PBS and harvested with ice-cold RIPA buffer (Beyotime Biotechnology, China) supplemented with complete protease inhibitor cocktail (Millipore Corporation). The cell lysates were centrifuged at 12,000 × *g* for 15 min at 4°C and the protein content of supernatant was determined using a BCA assay kit (Beyotime Biotechnology, China). Equivalent amounts of total proteins were separated by SDS-PAGE (10%) and transferred to polyvinylidene difluoride (PVDF) membranes. The membranes were blocked (5% fat-free milk powder in PBS with 0.1% Tween-20) at room temperature for 1 h. The membranes were then incubated with primary antibody including VSV-G, β-tubulin, ERK or phosphorylated-ERK at 4°C on a rocking shaker overnight. Subsequently, the membranes were washed 3 times with TBST buffer for 30 min (3×10 min) and incubated for 1 h with appropriate secondary antibody (diluted 1:10000 in blocking buffer) at room temperature. After washing, proteins were detected by enhanced chemiluminescence (Pierce Protein Research Products, Thermo Scientific) according to the manufacturer's instructions.

ERK1/2 MAP Kinase Phosphorylation assay

Phosphorylation of ERK1/2 MAP kinases was detected by protein immunoblotting using a phospho-ERK1/2-specific antibody (Cell Signaling Technology, Nottingham, UK). The PVDF membranes were stripped and re-probed using an anti-ERK1/2 antibody (Cell Signaling Technology) as a loading control.

Detection of Internalization (Fluorescence Microscopy) of H3R

Cells cultured on cover slips stably expressing an H3 receptor sensor were placed in a microscope chamber containing physiological HEPES-buffered saline solution (130 mM NaCl, 5 mM KCl, 1 mM $CaCl_2$, 1 mM $MgCl_2$, 20 mM HEPES, and 10 mM D-glucose, pH 7.4) and treated with 1×10^{-6} M imetit for different periods. The effect of CFP insertion on the distribution of receptors between the cell surface and cytoplasm was assessed by an inverted Olympus microscope.

Detection of Internalization (Biotinylation) of H3R

The stably transfected cells were grown and induced overnight with 100 ng/ml doxycycline in 6-well plates pre-coated with 0.1 mg/ml poly-D-lysine. Cells were then treated with specific ligands, as indicated. After treatment, plates were put on ice, the medium was removed and the cells were washed with ice cold borate buffer (10 mM boric acid, 154 mM NaCl, 7.2 mM KCl 1.8 mM $CaCl_2$, pH 9.0; 2 ml/well). Subsequently, 1 ml/well 0.8 mM Sulfo-NHS-SS-Biotin (Pierce, Thermo Scientific), in borate buffer, was added and the plates were incubated on ice in the dark for 30 min. After removing the biotin solution, the cells were washed with stop solution (192 mM glycine, 25 mM Tris-HCl, pH 8.3; 2 ml/well) and then incubated with 2 ml/well stop solution for 5 min on ice. Subsequently, the stop solution was removed and the cells were lysed by the addition of 500–1000 µl RIPA lysis buffer, and placed on ice for 15 min. The cell lysates were transferred to microcentrifuge tubes and centrifuged at 18,000× *g* for 10 min at 4 °C. Streptavidin-agarose resin (100 µl/tube) (Pierce, Thermo Scientific) was then added and tubes were incubated on a rotating wheel at 4 °C overnight followed by centrifugation at 2,000 ×*g* for 2 min at 4 °C. The supernatant was

removed and the resin was washed with 500 µl RIPA buffer three times. Subsequently, SDS-PAGE sample buffer (100 µl) containing 5% β-mercaptoethanol was added and tubes incubated at 37 °C for 1 h. The cell lysates and biotinylated samples were then subjected to SDS-PAGE and western blotting as described above.

Quantification of FRET efficiency

Cells induced to express the mGluR5-VSV-G-H3R-YFP-CFP construct were washed and placed into a microscope chamber containing physiological HEPES-buffered saline solution (130 mM NaCl, 5 mM KCl, 1 mM $CaCl_2$, 1 mM $MgCl_2$, 20 mM HEPES, and 10 mM D-glucose, pH7.4), and then imaged using an inverted Olympus IX83 micoscope (Olympus Instruments) equipped with a ×40 (numerical aperture = 1.3) oil immersion Fluor lens. Excitation light was generated from a computer-controlled Optoscan monochromator (TILL photonics, FEI, Germany), which was coupled to an ultra-highpoint intensity Optosource lamp, (TILL photonics) fitted with a 103-watt mercury arc lamp (Osram 103W/2). The monochromator was set to 427 nm with a bandwidth, (BW) of 5 nm or 504 nm/BW5 nm, to visualise cell surface located CFP-tagged receptors labelled with YFP. Excitation light, (427 nm or 504 nm), was reflected through the lens using a cyan/yellow fluorescent protein dual band dichroic filter (Semrock; Rochester, NY, catalogue no. FF440/520-Di01), mounted in the microscope. FRET and donor emission images were recorded at exactly the same time interval using a Quadview 2, (QV2), image splitting device (Photometrics, Canada), coupled to a CoolSnap-HQ2 camera connected to the microscope bottom port for maximal detection of emitted fluorescence. FRET and donor emission signals were detected simultaneously using the following Chroma (Chroma, Brattleboro, VT), ET series dichroic and emitters mounted in the QV2 cube: ET t505LPXR dichroic, ET535/30 nm, ET 470/30 nm. Using the streaming capability of the multiple dimensional wavelength acquisition module of MetaMorph, ligand-induced changes in intramolecular FRET were recorded at 40 ms intervals during excitation with 427 nm light directly to the computer hard drive. The Cool Snap-HQ2 camera was operated in 14-bit mode and exposure time, binning (8 × 8), and camera gain, were kept constant for all streaming experiments. Computer control of all electronic hardware and camera streaming acquisition was achieved using Metamorph software (version 7.7.5 Molecular

Devices, Sunnydale, CA). TTL controlled solenoid valves connected to a peristaltic pump operated at a flow rate of 5 ml/min were used to rapidly add or remove test ligands to or from the imaging chamber. Cells were treated for 1 minute in total, in detail, the cells were first treated with HEPES-buffer for 15 sec, then with different concentration of agonists for 15 sec, and finally with HEPES-buffer for 30 sec. In our FRET assay experiments the quantification of FRET efficiency is dependent upon the distance between two interacting fluorescence dipoles, therefore ligand evoked changes in the conformational state of the receptor will alter FRET efficiency. All of the intracellular FRET assays were performed with a fixed acceptor to donor stoichiometry, therefore the ratio of acceptor emission to donor emission was used to measure the relative FRET efficiency (ratiometric FRET), which eliminated the need to correct for fluorescence bleed through contamination. A CFP-YFP tandem reference construct with known FRET efficiency was used for calibration in each experiment, and all analyses of acquired images were performed using MetaMorph software (Molecular Devices). Ratiometric FRET region of interest values were then calculated as the average 535 nm emission intensity divided by the average 470 nm emission intensity. The quantified FRET ratios were exported to Prism 5.02 (GraphPad Software Inc.) and the baseline FRET ratio was normalised to 1.0 using the transforming module of the software and plotted over time.

Performance of acceptor photobleaching

Resonance energy transfer was quantified using the FRET acceptor photobleaching method described by Kenworthy [70], whereby high intensity laser illumination photobleaching destruction of the acceptor (YFP) will convert the donor from a quenched to an unquenched state and a significant increase in fluorescence of the donor (CFP) will be observed in the recorded post bleach donor channel sequence of images.

An invert Nikon A1R confocal microscope (Nikon, Dusseldorf, Germany), equipped with the laser lines 440 nm and 514 nm were operated at low power intensity (0.15%), to ensure that the collection of the pre-bleach (n = 5), and post-bleach (n = 5), set of donor (emission set to 470 nm), and acceptor (emission set to 535 nm), images did not suffer significantly from masked photobleaching issues prior to ROI selective photobleaching destruction of the acceptor fluorescent protein to eliminate resonance energy transfer from the donor to the acceptor. Selective ROI photobleaching illumination destruction of the acceptor was achieved by setting the laser power of the 514 nm laser line to 75% power intensity (95 mW laser power at the specimen), and the selected ROI drawn on the acceptor channel image was repeatedly scanned 20 times using these bleaching illumination conditions prior to acquisition of the post bleach donor and acceptor image sets. The objective lens used for imaging the cells was a ×40 oil immersion fluor objective (NA = 1.3) and images were collected using 2× zoom to the middle of the cell. FRET efficiency (E) was quantified by using the following formula:

E = 1 – (Prebleach Donor ROI fluorescent intensity / (Postbleach Donor ROI fluorescent intensity.

Receptor Activation Switch Kinetic Data Analysis

Baseline fluorescence was measured for 15 seconds before ligand addition and ligand-driven fluorescence changes were measured until they reached a plateau, (i.e. 15 secs after ligand addition). All data were corrected for fluid superfusion dead space, (15 secs), and curve fit analysis was performed using Prism 5.01 (GraphPad Software Inc., San Diego, CA). Ligand driven, concentration dependent time course changes in the rate of rise of the FRET ratio signal, (e.g. Kon = observed ligand driven receptor activation switch kinetics), were quantified using Graphpad's one phase exponential association algorithm. Rate of decrease in the FRET signal upon ligand removal was measured by fitting a mono-exponential dissociation algorithm (Koff). All values are given as mean $\pm$ S.E.M. of n independent experiments. Statistical comparisons between parameters were performed using Student's *t* test, with $p < 0.05$ taken as indicating significance.

Cell membrane preparation

H3R biosensor stable expression cells were grown to 80-90% confluency in 150 cm^2 cell-culture plates with doxycycline induction as required. The cell-culture media was removed and the monolayer briefly washed with ice-cold HBS-EDTA (2 × 10 ml; 10mM HEPES, 0.9% w v^{-1} NaCl, 0.2% w v^{-1} EDTA pH7.4). All subsequent steps were conducted at 4°C to avoid receptor degradation. HBS-EDTA (10 ml) was added and left for approximately 20 min for the cells to detach from the culture substrate. The cells were then removed from the plates into a 50 ml centrifuge tube and subsequently centrifuged at 250 × *g* for 5 min to allow a pellet to form. The supernatant fraction was aspirated and 20 ml per 150 cm^2 tray of wash buffer 1 (10 mM HEPES, 10 mM EDTA, pH 7.4) was added to the pellet. This was homogenised using a Polytron (20,000 RPM, 5 × 10 s bursts) and subsequently centrifuged at 50,000 × *g* at 4 °C for 5 min. The supernatant fraction was colletcted and the pellet rehomogenised and centrifuged at 50,000 × *g* at 4 °C for 15 min in wash buffer 2 (10 mM HEPES, 0.1 mM EDTA, pH 7.4). The final pellet was suspended in wash buffer 2, protein concentration was assessed and membranes were stored at -80 °C until required.

[^{3}H]-histamine saturation binding assays (membrane)

Binding was established by the addition of 10 μg of membrane protein to assay buffer (25 mM HEPES, 0.5 mM EDTA, and 2.5 mM $MgCl_2$, pH7.4, supplemented with 0.3% BSA) containing varying concentrations of [^{3}H]-histamine (0.4–16 nM). Reaction were incubated for 90 min at 25 °C, and bound ligand was separated from free by vacuum filtration through GF/C filters (Brandel Inc, Gaithersbrug, MD). The filters were washed twice with cold assay buffer and transfer filter disks to scintillation vials, add scintillant, and then counted by using Multi-Purpose Scientillation Counter (BECKMAN COULTER LS6500, USA). The bound ligand was estimated by liquid scintillation spectrometry.

[^{3}H]-histamine saturation binding assays (intact cells)

Cells were grown overnight, with doxycycline induction as required, on white 96-well plates, which had been treated with 0.1 mg ml^{-1} poly-D-lysine. The medium was removed and replaced with 200 µl per well buffer containing 150 mM NaCl, 20 mM HEPES and 0.5% BSA, pH 7.4 with varying concentrations of [^{3}H]-histamine (0.4–16 nM). The plates were incubated at 25 °C for 60 min and terminated by removal of the binding mixture, followed by washing with 3 × 200 µl per well, ice-cold 1 × PBS. The plates sealed before incubation for 2 h at room temperature on a rapidly shaking platform. Using the specific binding per well and the number of cells per well, mol [^{3}H]-histamine cell^{-1} was determined.

[^{3}H]-histamine competition binding assays

For competition binding assays, the concentration of [^{3}H]-histamine was 10 nM, and three different concentrations of unlabeled ligand were co-added simultaneously. At the indicated time points, 10 µg of membrane protein was added and incubated with 0 - 270 min time points. Three different concentrations of competitor were assessed to ensure that the rate parameters calculated were independent of ligand concentration.

Determination of the observed association rate (Kob) of [^{3}H]-histamine

To determine the Kon accurately, the Kob of [^{3}H]-histamine was calculated at the concentration of 10 nM. The experiment was initiated (t = 0) by the addition of [^{3}H]-histamine to H3R stable expression cell membranes (10 µg well^{-1}) in assay binding buffer (final assay volume 500 µl) and incubated with 0 - 270 min time points. All samples were then processed simultaneously. Free [^{3}H]-histamine was separated at multiple time points to construct association kinetic curves. After incubation, bound was separated from free by rapid filtration, plates were left to dry and radioactivity quantified.

Determination of the dissociation rate (Koff) of [^{3}H]-histamine

The dissociation rate of [^{3}H]-histamine was determined by allowing approximately 10 nM [^{3}H]-histamine (exact concentration determined for each experiment using liquid scintillation counting) to reach equilibrium with H3R stable expression cell membranes (10 µg well^{-1}) in a final volume of 500 µl. Equilibrium was verified by harvesting an identical plate before the start of the experiment and then comparing total binding on this plate to that on the proceeding plates. After equilibrium was reached (approximately 1 h), reassociation of [^{3}H]-histamine was prevented by the addition of 1.5 ml clobenpropit (1 µM final). The moment of clobenpropit addition was considered as *t* = 0 and bound [^{3}H]-histamine was measured at multiple time points post *t* = 0. Care was taken to ensure that [^{3}H]-histamine was fully dissociated from the H3 receptor. Dissociation data were fitted to a single-phase exponential decay function and the $t_{1/2}$ value obtained was transformed into a Koff rate using Equation 1:

$$\text{Koff} = \frac{0.693}{t_{1/2}} \qquad (1)$$

[^{3}H]-histamine association data were fitted to a single-phase exponential association function to calculate an observed rate constant Kob. The association rate constant, Kon, was calculated using Equation 2, as described originally by Hill [71]:

$$\text{Kon} = \frac{(\text{Kob} - \text{Koff})}{[\text{radioligand}]} \qquad (2)$$

Where the Koff value used was predetermined from dissociation rate experiments.

Author contributions

Tian-Rui Xu and Ying Liu performed data analysis, discussed the results and wrote the manuscript. Hong Zeng and John D. Pediani contributed to FRET sensors construction and biological activities analysis. Richard J. Ward, Yang Yang and Su An contributed to revise the manuscript. Lu-Yao Chen, Nan Wu, Li Ma and Mei Tang contributed to cell culture and molecular biological analysis. Xiao-Xi

Guo and Qian Hao gave help in the analysis and discussion. All authors have read and approved the final manuscript.

Conflict of interest statement

The authors declare no conflicts of interest.

Acknowledgments

This work was funded NSFC funding (81473342, 81560455, 81460417, 81460253, 81760264, 31660099, U1302225) and High-End Talent Grant of Yunnan Province, China (2012HA008). Most of experiments are conducted in University Based Provincial Key Laboratory of Screening and Utilization of Targeted Drugs, key laboratory of sustainable utilization of *Panax notoginseng* of Yunnan province, the [^{3}H]-histamine radioligand experiment was performed by Isotype Laboratory of Nanjing Agriculture University.

References

1. Feuerstein, T. J. (2008) Presynaptic receptors for dopamine, histamine, and serotonin, *Handbook of experimental pharmacology*, 289-338.

2. Osorio-Espinoza, A., Alatorre, A., Ramos-Jimenez, J., Garduno-Torres, B., Garcia-Ramirez, M., Querejeta, E. & Arias-Montano, J. A. (2011) Pre-synaptic histamine H(3) receptors modulate glutamatergic transmission in rat globus pallidus, *Neuroscience.* **176**, 20-31.

3. Panula, P. & Nuutinen, S. (2013) The histaminergic network in the brain: basic organization and role in disease, *Nature reviews Neuroscience.* **14**, 472-87.

4. Haas, H. L., Sergeeva, O. A. & Selbach, O. (2008) Histamine in the nervous system, *Physiological reviews.* **88**, 1183-241.

5. Molina-Hernandez, A., Nunez, A., Sierra, J. J. & Arias-Montano, J. A. (2001) Histamine H3 receptor activation inhibits glutamate release from rat striatal synaptosomes, *Neuropharmacology.* **41**, 928-34.

6. Parmentier, R., Anaclet, C., Guhennec, C., Brousseau, E., Bricout, D., Giboulot, T., Bozyczko-Coyne, D., Spiegel, K., Ohtsu, H., Williams, M. & Lin, J. S. (2007) The brain H3-receptor as a novel therapeutic target for vigilance and sleep-wake disorders, *Biochemical pharmacology.* **73**, 1157-71.

7. Brioni, J. D., Esbenshade, T. A., Garrison, T. R., Bitner, S. R. & Cowart, M. D. (2011) Discovery of histamine H3 antagonists for the treatment of cognitive disorders and Alzheimer's disease, *The Journal of pharmacology and experimental therapeutics.* **336**, 38-46.

8. Medhurst, A. D., Atkins, A. R., Beresford, I. J., Brackenborough, K., Briggs, M. A., Calver, A. R., Cilia, J., Cluderay, J. E., Crook, B., Davis, J. B., Davis, R. K., Davis, R. P., Dawson, L. A., Foley, A. G., Gartlon, J., Gonzalez, M. I., Heslop, T., Hirst, W. D., Jennings, C., Jones, D. N., Lacroix, L. P., Martyn, A., Ociepka, S., Ray, A., Regan, C. M., Roberts, J. C., Schogger, J., Southam, E., Stean, T. O., Trail, B. K., Upton, N., Wadsworth, G., Wald, J. A., White, T., Witherington, J., Woolley, M. L., Worby, A. & Wilson, D. M. (2007) GSK189254, a novel H3 receptor antagonist that binds to histamine H3 receptors in Alzheimer's disease brain and improves cognitive performance in preclinical models, *The Journal of pharmacology and experimental therapeutics.* **321**, 1032-45.

9. Raddatz, R., Tao, M. & Hudkins, R. L. (2010) Histamine H3 antagonists for treatment of cognitive deficits in CNS diseases, *Current topics in medicinal chemistry.* **10**, 153-69.

10. Dauvilliers, Y., Bassetti, C., Lammers, G. J., Arnulf, I., Mayer, G., Rodenbeck, A., Lehert, P., Ding, C. L., Lecomte, J. M., Schwartz, J. C. & group, H. I. s. (2013) Pitolisant versus placebo or modafinil in patients with narcolepsy: a double-blind, randomised trial, *The Lancet Neurology.* **12**, 1068-75.

11. Bongers, G., Bakker, R. A. & Leurs, R. (2007) Molecular aspects of the histamine H3 receptor, *Biochemical pharmacology.* **73**, 1195-204.

12. Takeshita, Y., Watanabe, T., Sakata, T., Munakata, M., Ishibashi, H. & Akaike, N. (1998) Histamine modulates high-voltage-activated calcium channels in neurons dissociated from the rat tuberomammillary nucleus, *Neuroscience.* **87**, 797-805.

13. Nieto-Alamilla, G., Marquez-Gomez, R., Garcia-Galvez, A. M., Morales-Figueroa, G. E. & Arias-Montano, J. A. (2016) The Histamine H3 Receptor: Structure, Pharmacology, and Function, *Molecular pharmacology.* **90**, 649-673.

14. Drutel, G., Peitsaro, N., Karlstedt, K., Wieland, K., Smit, M. J., Timmerman, H., Panula, P. & Leurs, R. (2001) Identification of rat H3 receptor isoforms with different brain expression and signaling properties, *Molecular pharmacology.* **59**, 1-8.

15. Giovannini, M. G., Efoudebe, M., Passani, M. B., Baldi, E., Bucherelli, C., Giachi, F., Corradetti, R. & Blandina, P. (2003) Improvement in fear memory by histamine-elicited ERK2 activation in hippocampal CA3 cells, *The Journal of neuroscience : the official journal of the Society for Neuroscience.* **23**, 9016-23.

16. Storch, U., Straub, J., Erdogmus, S., Gudermann, T. & Mederos, Y. S. M. (2017) Dynamic monitoring of Gi/o-protein-mediated decreases of intracellular cAMP by FRET-based Epac sensors, *Pflugers Archiv : European journal of physiology.* **469**, 725-737.

17. Pennock, R. L. & Hentges, S. T. (2016) Desensitization-resistant and -sensitive GPCR-mediated inhibition of GABA release occurs by Ca2+-dependent and -independent mechanisms at a hypothalamic synapse, *Journal of neurophysiology.* **115**, 2376-88.

18. Jain, R., Watson, U. & Saini, D. K. (2016) ERK activated by Histamine H1 receptor is anti-proliferative through spatial restriction in the cytosol, *European journal of cell biology.* **95**, 623-634.

19. Alex, A. & Antunes, A. (2015) Pyrosequencing characterization of the microbiota from Atlantic intertidal marine sponges reveals high microbial diversity and the lack of co-occurrence patterns, *PloS one.* **10**, e0127455.

20. Soethoudt, M., van Gils, N., van der Stelt, M. & Heitman, L. H. (2016) Protocol to Study beta-Arrestin Recruitment by CB1 and CB2 Cannabinoid Receptors, *Methods in molecular biology.* **1412**, 103-11.

21. Jares-Erijman, E. A. & Jovin, T. M. (2003) FRET imaging, *Nature biotechnology.* **21**, 1387-95.

22. Hoffmann, C., Gaietta, G., Bunemann, M., Adams, S. R., Oberdorff-Maass, S., Behr, B., Vilardaga, J. P., Tsien, R. Y., Ellisman, M. H. & Lohse, M. J. (2005) A FlAsH-based FRET approach to determine G protein-coupled receptor activation in living cells, *Nature methods.* **2**, 171-6.

23. Maier-Peuschel, M., Frolich, N., Dees, C., Hommers, L. G., Hoffmann, C., Nikolaev, V. O. & Lohse, M. J. (2010) A fluorescence resonance energy transfer-based M2 muscarinic receptor sensor reveals rapid kinetics of allosteric modulation, *The Journal of biological chemistry.* **285**, 8793-800.

24. Alvarez-Curto, E., Prihandoko, R., Tautermann, C. S., Zwier, J. M., Pediani, J. D., Lohse, M. J., Hoffmann, C., Tobin, A. B. & Milligan, G. (2011) Developing chemical genetic approaches to explore G protein-coupled receptor function: validation of the use of a receptor activated solely by synthetic ligand (RASSL), *Molecular pharmacology.* **80**, 1033-46.

25. Jensen, J. B., Lyssand, J. S., Hague, C. & Hille, B. (2009) Fluorescence changes reveal kinetic steps of muscarinic receptor-mediated modulation of phosphoinositides and Kv7.2/7.3 K+ channels, *The Journal of general physiology.* **133**, 347-59.

26. Markovic, D., Holdich, J., Al-Sabah, S., Mistry, R., Krasel, C., Mahaut-Smith, M. P. & Challiss, R. A. (2012) FRET-based detection of M1 muscarinic acetylcholine receptor activation by orthosteric and allosteric agonists, *PloS one.* **7**, e29946.

27. Fernandez-Duenas, V., Gomez-Soler, M., Lopez-Cano, M., Taura, J. J., Ledent, C., Watanabe, M., Jacobson, K. A., Vilardaga, J. P. & Ciruela, F. (2014) Uncovering caffeine's adenosine A2A receptor inverse agonism in experimental parkinsonism, *ACS chemical biology.* **9**, 2496-501.

28. Candelario J, C. M. (2012) Mechanical stress stimulates

conformational changes in 5-hydroxytryptamine receptor 1B in bone

cells. , *Cel Mol Bioeng.* **5**, 277-286.

29. Xu, T. R., Ward, R. J., Pediani, J. D. & Milligan, G. (2012) Intramolecular fluorescence resonance energy transfer (FRET) sensors of the orexin OX1 and OX2 receptors identify slow kinetics of agonist activation, *The Journal of biological chemistry.* **287**, 14937-49.

30. van Unen, J., Woolard, J., Rinken, A., Hoffmann, C., Hill, S. J., Goedhart, J., Bruchas, M. R., Bouvier, M. & Adjobo-Hermans, M. J. (2015) A Perspective on Studying G-Protein-Coupled Receptor Signaling with Resonance Energy Transfer Biosensors in Living Organisms, *Molecular pharmacology.* **88**, 589-95.

31. Guo, J., Sachs, F. & Meng, F. (2014) Fluorescence-based force/tension sensors: a novel tool to visualize mechanical forces in structural proteins in live cells, *Antioxidants & redox signaling.* **20**, 986-99.

32. Meng, F., Suchyna, T. M., Lazakovitch, E., Gronostajski, R. M. & Sachs, F. (2011) Real Time FRET Based Detection of Mechanical Stress in Cytoskeletal and Extracellular Matrix Proteins, *Cellular and molecular bioengineering.* **4**, 148-159.

33. Meng, F., Suchyna, T. M. & Sachs, F. (2008) A fluorescence energy transfer-based mechanical stress sensor for specific proteins in situ, *The FEBS journal.* **275**, 3072-87.

34. Audet, M. & Bouvier, M. (2012) Restructuring G-protein- coupled receptor activation, *Cell.* **151**, 14-23.

35. Kobilka, B. K. (2007) G protein coupled receptor structure and activation, *Biochimica et biophysica acta.* **1768**, 794-807.

36. Lindenburg, L. & Merkx, M. (2014) Engineering genetically encoded FRET sensors, *Sensors.* **14**, 11691-713.

37. Ward, R. J., Alvarez-Curto, E. & Milligan, G. (2011) Using the Flp-In T-Rex system to regulate GPCR expression, *Methods Mol Biol.* **746**, 21-37.

38. Luttrell, L. M. & Gesty-Palmer, D. (2010) Beyond desensitization: physiological relevance of arrestin-dependent signaling, *Pharmacological reviews.* **62**, 305-30.

39. Hamamoto, A., Yamato, S., Katoh, Y., Nakayama, K., Yoshimura, K., Takeda, S., Kobayashi, Y. & Saito, Y. (2016) Modulation of primary cilia length by melanin-concentrating hormone receptor 1, *Cellular signalling.* **28**, 572-84.

40. Glaser, R. W. (1993) Antigen-antibody binding and mass transport by convection and diffusion to a surface: a two-dimensional computer model of binding and dissociation kinetics, *Analytical biochemistry.* **213**, 152-61.

41. Palau, W. & Di Primo, C. (2012) Single-cycle kinetic analysis of ternary DNA complexes by surface plasmon resonance on a decaying surface, *Biochimie.* **94**, 1891-9.

42. Jacobsen, S. E., Ammendrup-Johnsen, I., Jansen, A. M., Gether, U., Madsen, K. L. & Brauner-Osborne, H. (2017) The GPRC6A receptor displays constitutive internalization and sorting to the slow recycling pathway, *The Journal of biological chemistry.* **292**, 6910-6926.

43. Shi, Y., Sheng, R., Zhong, T., Xu, Y., Chen, X., Yang, D., Sun, Y., Yang, F., Hu, Y. & Zhou, N. (2012) Identification and characterization of ZEL-H16 as a novel agonist of the histamine H3 receptor, *PloS one.* **7**, e42185.

44. Mele, T. & Juric, D. M. (2013) Identification and pharmacological characterization of the histamine H3 receptor in cultured rat astrocytes, *European journal of pharmacology.* **720**, 198-204.

45. Morales-Figueroa, G. E., Marquez-Gomez, R., Gonzalez-Pantoja, R., Escamilla-Sanchez, J. & Arias-Montano, J. A. (2014) Histamine H3 receptor activation counteracts adenosine A2A receptor-mediated enhancement of depolarization-evoked [3H]-GABA release from rat globus pallidus synaptosomes, *ACS chemical neuroscience.* **5**, 637-45.

46. Liu, C., Ma, X., Jiang, X., Wilson, S. J., Hofstra, C. L., Blevitt, J., Pyati, J., Li, X., Chai, W., Carruthers, N. & Lovenberg, T. W. (2001) Cloning and pharmacological characterization of a fourth histamine receptor (H(4)) expressed in bone marrow, *Molecular pharmacology.* **59**, 420-6.

47. Wieland, K., Bongers, G., Yamamoto, Y., Hashimoto, T., Yamatodani, A., Menge, W. M., Timmerman, H., Lovenberg, T. W. & Leurs, R. (2001) Constitutive activity of histamine h(3) receptors stably expressed in SK-N-MC cells: display of agonism and inverse agonism by H(3) antagonists, *The Journal of pharmacology and experimental therapeutics.* **299**, 908-14.

48. Wulff, B. S., Hastrup, S. & Rimvall, K. (2002) Characteristics of recombinantly expressed rat and human histamine H3 receptors, *European journal of pharmacology.* **453**, 33-41.

49. Coge, F., Guenin, S. P., Audinot, V., Renouard-Try, A., Beauverger, P., Macia, C., Ouvry, C., Nagel, N., Rique, H., Boutin, J. A. & Galizzi, J. P. (2001) Genomic organization and characterization of splice variants of the human histamine H3 receptor, *The Biochemical journal.* **355**, 279-88.

50. Kitbunnadaj, R., Zuiderveld, O. P., De Esch, I. J., Vollinga, R. C., Bakker, R., Lutz, M., Spek, A. L., Cavoy, E., Deltent, M. F., Menge, W. M., Timmerman, H. & Leurs, R. (2003) Synthesis and structure-activity relationships of conformationally constrained histamine H(3) receptor agonists, *Journal of medicinal chemistry.* **46**, 5445-57.

51. van Unen, J., Yin, T., Wu, Y. I., Mastop, M., Gadella, T. W., Jr. & Goedhart, J. (2016) Kinetics of recruitment and allosteric activation of ARHGEF25 isoforms by the heterotrimeric G-protein Galphaq, *Scientific reports.* **6**, 36825.

52. Langmead, C. J., Jerman, J. C., Brough, S. J., Scott, C., Porter, R. A. & Herdon, H. J. (2004) Characterisation of the binding of [3H]-SB-674042, a novel nonpeptide antagonist, to the human orexin-1 receptor, *British journal of pharmacology.* **141**, 340-6.

53. Ward, R. J., Pediani, J. D. & Milligan, G. (2011) Heteromultimerization of cannabinoid CB(1) receptor and orexin OX(1) receptor generates a unique complex in which both protomers are regulated by orexin A, *The Journal of biological chemistry.* **286**, 37414-28.

54. Ward, R. J., Pediani, J. D. & Milligan, G. (2011) Ligand-induced internalization of the orexin OX(1) and cannabinoid CB(1) receptors assessed via N-terminal SNAP and CLIP-tagging, *British journal of pharmacology.* **162**, 1439-52.

55. Esbenshade, T. A., Krueger, K. M., Miller, T. R., Kang, C. H., Denny, L. I., Witte, D. G., Yao, B. B., Fox, G. B., Faghih, R., Bennani, Y. L., Williams, M. & Hancock, A. A. (2003) Two novel and selective nonimidazole histamine H3 receptor antagonists A-304121 and A-317920: I. In vitro pharmacological effects, *The Journal of pharmacology and experimental therapeutics.* **305**, 887-96.

56. Bouaboula, M., Perrachon, S., Milligan, L., Canat, X., Rinaldi-Carmona, M., Portier, M., Barth, F., Calandra, B., Pecceu, F., Lupker, J., Maffrand, J. P., Le Fur, G. & Casellas, P. (1997) A selective inverse agonist for central cannabinoid receptor inhibits mitogen-activated protein kinase activation stimulated by insulin or insulin-like growth factor 1. Evidence for a new model of receptor/ligand interactions, *The Journal of biological chemistry.* **272**, 22330-9.

57. Kuramasu, A., Sukegawa, J., Sato, T., Sakurai, E., Watanabe, T., Yanagisawa, T. & Yanai, K. (2011) The hydrophobic amino acids in putative helix 8 in carboxy-terminus of histamine H(3) receptor are involved in receptor-G-protein coupling, *Cellular signalling.* **23**, 1843-9.

58. Leurs, R., Bakker, R. A., Timmerman, H. & de Esch, I. J. (2005) The histamine H3 receptor: from gene cloning to H3 receptor drugs, *Nature reviews Drug discovery.* **4**, 107-20.

59. Ziegler, N., Batz, J., Zabel, U., Lohse, M. J. & Hoffmann, C. (2011) FRET-based sensors for the human M1-, M3-, and M5-acetylcholine receptors, *Bioorganic & medicinal chemistry.* **19**, 1048-54.

60. Nguyen, T., Shapiro, D. A., George, S. R., Setola, V., Lee, D. K., Cheng, R., Rauser, L., Lee, S. P., Lynch, K. R., Roth, B. L. & O'Dowd, B. F. (2001) Discovery of a novel member of the histamine receptor family, *Molecular pharmacology.* **59**, 427-33.

61. Wang, J. Y., Chen, S. P., Gao, Y. H., Qiao, L. N., Zhang, J. L. & Liu, J. L. (2015) Effect of Repeated Electroacupuncture Intervention on Hippocampal ERK and p38MAPK Signaling in Neuropathic Pain Rats, *Evidence-based complementary and alternative medicine : eCAM.* **2015**, 641286.

62. Chen, W. F., Wu, L., Du, Z. R., Chen, L., Xu, A. L., Chen, X. H., Teng, J. J. & Wong, M. S. (2017) Neuroprotective properties of icariin in MPTP-induced mouse model of Parkinson's disease: Involvement of PI3K/Akt and MEK/ERK signaling pathways, *Phytomedicine : international journal of phytotherapy and phytopharmacology.* **25**, 93-99.

63. Johansson, D. X., Brismar, H. & Persson, M. A. (2007) Fluorescent protein pair emit intracellular FRET signal suitable for FACS screening, *Biochemical and biophysical research communications.* **352**, 449-55.

64. Ayoub, M. A., Maurel, D., Binet, V., Fink, M., Prezeau, L., Ansanay, H. & Pin, J. P. (2007) Real-time analysis of agonist-induced activation of protease-activated receptor 1/Galphai1 protein complex measured by bioluminescence resonance energy transfer in living cells, *Molecular pharmacology.* **71**, 1329-40.

65. Lohse, M. J., Nuber, S. & Hoffmann, C. (2012) Fluorescence/bioluminescence resonance energy transfer techniques to study G-protein-coupled receptor activation and signaling, *Pharmacological reviews.* **64**, 299-336.

66. Stoddart, L. A., Johnstone, E. K., Wheal, A. J., Goulding, J., Robers, M. B., Machleidt, T., Wood, K. V., Hill, S. J. & Pfleger, K. D. (2015) Application of BRET to monitor ligand binding to GPCRs, *Nature methods.* **12**, 661-3.

67. Stoddart, L. A., White, C. W., Nguyen, K., Hill, S. J. & Pfleger, K. D. (2016) Fluorescence- and bioluminescence-based approaches to study GPCR ligand binding, *British journal of pharmacology.* **173**, 3028-37.

68. Vernall, A. J., Hill, S. J. & Kellam, B. (2014) The evolving small-molecule fluorescent-conjugate toolbox for Class A GPCRs, *British journal of pharmacology.* **171**, 1073-84.

69. Zwier, J. M., Roux, T., Cottet, M., Durroux, T., Douzon, S., Bdioui, S., Gregor, N., Bourrier, E., Oueslati, N., Nicolas, L., Tinel, N., Boisseau, C., Yverneau, P., Charrier-Savournin, F., Fink, M. & Trinquet, E. (2010) A fluorescent ligand-binding alternative using Tag-lite(R) technology, *Journal of biomolecular screening.* **15**, 1248-59.

70. Kenworthy, A. K. (2001) Imaging protein-protein interactions using fluorescence resonance energy transfer microscopy, *Methods.* **24**, 289-96.

71. Hill, A. V. (1909) The mode of action of nicotine and curari, determined by the form of the contraction curve and the method of temperature coefficients, *The Journal of physiology.* **39**, 361-73.

Table.1 Association and dissociation rate constants (Kon, Koff) and dissociation constant (Kd) determined with FRET sensor

	Histamine (M)				
	10^{-5}	10^{-6}	10^{-7}	10^{-8}	10^{-9}
Kon ($10^5 M^{-1}s^{-1}$)	0.55 ± 0.12	0.55 ± 0.04	0.50 ± 0.03	0.44 ± 0.05	0.30 ± 0.10
Koff ($10^{-3}s^{-1}$)	0.20 ± 0.08	0.20 ± 0.11	0.19 ± 0.07	0.16 ± 0.07	0.11 ± 0.08
Kd (nM)	3.60 ± 0.06	3.53 ± 0.05	3.87 ± 0.11	3.73 ± 0.04	3.72 ± 0.06
	Imetit (M)				
	10^{-5}	10^{-6}	10^{-7}	10^{-8}	10^{-9}
Kon ($10^5 M^{-1}s^{-1}$)	0.62 ± 0.13*	0.59 ± 0.02	0.58 ± 0.10	0.53 ± 0.05	0.53 ± 0.07*
Koff ($10^{-3}s^{-1}$)	0.29 ± 0.05*	0.29 ± 0.06*	0.27 ± 0.12*	0.25 ± 0.03*	0.24 ± 0.04*
Kd (nM)	4.72 ± 0.06	4.81 ± 0.07	4.75 ± 0.03	4.75 ± 0.01	4.57 ± 0.06

Data represent the mean ± S.E.M. of five experiments performed in duplicate. Kon, the associations rate constant; Koff, the disociation rate constant; Kd is then calculated as the Koff/Kon ratio.

* significantly different (p<0.05) from the histamine treatment and imetit treatment as determined by one-way ANOVA followed by Dunnett's post test.

.

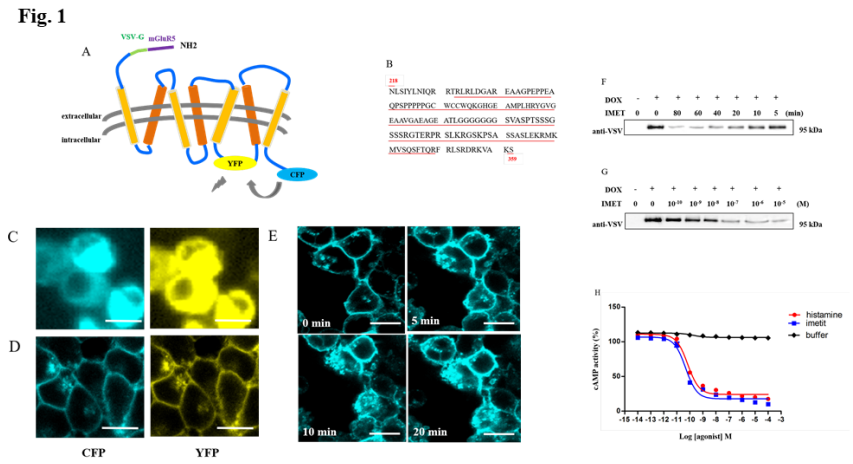

Figure 1. Design and expression of an H3R FRET sensor and its internalization in response to imetit treatment. A. Cartoon to show the human H3 receptor modified at the N-terminus by the addition of a leader sequence from the metabotropic glutamate 5 receptor (mGluR5) followed by the VSV-G peptide epitope sequence, whilst enhanced cyan fluorescent protein (CFP) was fused in-frame to the C-terminus. YFP was introduced into the third intracellular loop which links transmembrane domains V and VI. Energy transfer from CFP to YFP and subsequent output is illustrated. **B**. Amino acid sequence of the intracellular loop 3 of human H3 receptor. In the sensors used in this study, the YFP motif replaced the sequence underlined in red, with both ends of the loop retaining 12 amino acids. **C**. The plasmid construct was transiently transfected into HEK293 cells and the expression of CFP and YFP fluorescence was observed. Scale bar 10 µm. **D**. The construct was cloned into the Flp-In locus of Flp-In ™ T-REx ™ HEK 293 cells and expression induced by addition of doxycycline, imaging of CFP or YFP showed effective delivery of this sensor to the cell surface. Scale bar 10 µm. **E**. Flp-In™ T-REx™ HEK 293 cells induced to express mGluR5-VSV-G-H3R-YFP-CFP were imaged to detect CFP at various times following addition of imetit (1×10^{-6} M). Scale bar 10 µm. **F** and **G**. Cell surface biotinylation studies were performed on Flp-In™ T-REx™ HEK 293 cells harboring the mGluR5-VSV-G-H3R-YFP-CFP construct that was either doxycycline-induced, or not, to express the sensor. The induced cells were treated with 1×10^{-6} M imetit for varying times (**F**) or different concentrations of imetit were added for 40 min (**G**). Cell surface biotinylated proteins were captured, resolved by SDS-PAGE, and mGluR5-VSV-G-H3R-YFP-CFP was detected by immunoblotting with anti-VSV-G. Imetit induced internalization, and therefore, reduced the amount of cell surface mGluR5-VSV-G-H3R-YFP-CFP available to be biotinylated, in a time- and concentration-dependent manner. Representative examples are shown of *n*=3 independent experiments. **H**. cAMP accumulation in cells of H3R FRET

sensor was measured by using a cAMP assay kit. Concentration-response curves for histamine (blue) and imetit (red) are presented. Data shown are from three experiments, data points are mean ± S.E.M., *n* =3. Data were analysed by non-linear regression and were best fit to a sigmoidal concentration response curve.

Fig. 2

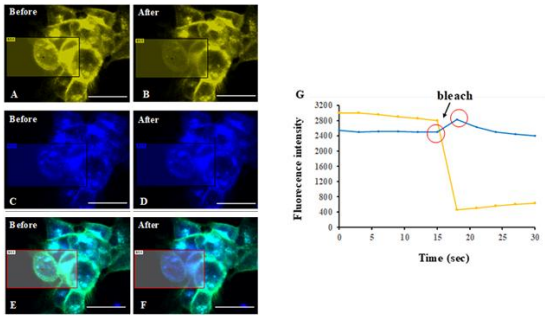

Figure 2. Acceptor photobleaching of cells stable expression of a CFP-YFP fusion. A-D, a YFP-image and a CFP-image before bleaching (A and C) or after bleaching (B and D). (E) CFP (donor) channel before the bleach and (F) CFP (donor) channel after the bleach. No dramatic change in CFP fluorescence is observed in the zones bleached by the 514 laser line (red square in (F) vs. (E)). (G) Quantification of fluorescent intensity in a representative example shows an increase in fluorescence after the bleach. Scale bar 10 µm.

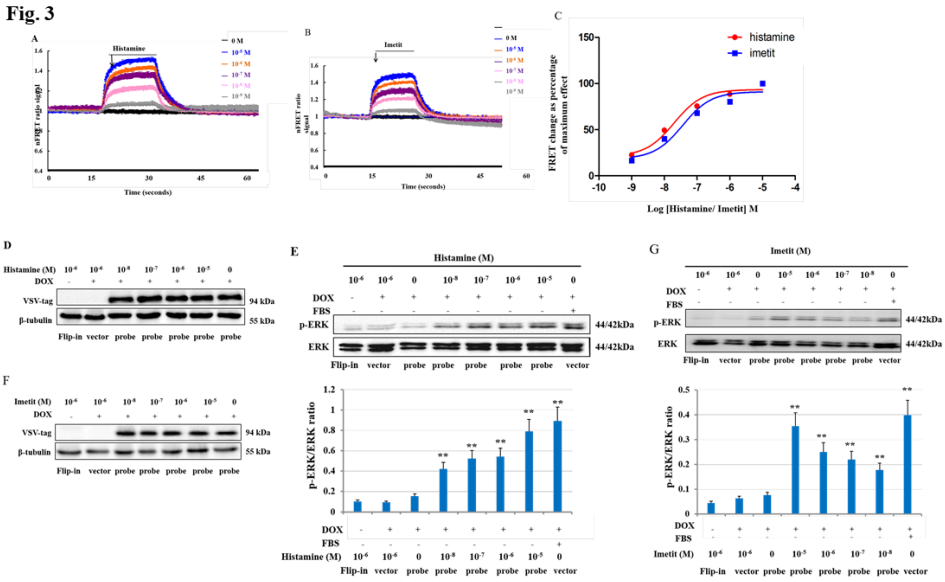

Figure 3. Response of an H3 intramolecular FRET sensor to histamine or imetit is both time- and dose-dependent. Flp-In™ T-REx™ 293 cells induced to express mGluR5-VSV-G-H3R-YFP-CFP were used for FRET imaging studies. **A** and **B**, various concentrations of histamine (**A**) or imetit (**B**) were added at the indicated point and the FRET signal monitored over the ensuing 15 s period. Agonist was removed after application for 15 s. **C**. Change in normalized FRET signal due to addition of the ligands at the 15 s time point was measured and normalized against the effect of 10^{-5} M histamine or imetit, defined as 100%, or vehicle, defined as 0%. The H3R intramolecular sensor cells were treated with various concentrations of histamine (**D**) or imetit (**F**) for 5 min. The effects of histamine or imetit on the expression of the construct were assessed by western blotting. The H3R intramolecular sensor cells were serum-starved for 12 h, stimulated with various concentrations of histamine (**E**) or imetit (**G**) for 5 min, and the expression of phosphorylated ERK (p-ERK) and total ERK was analysed by western blotting. Flp-in: Flp-In™ T-REx™ 293 cells; vector: pcDNA5/FRT/To vector; probe: p5-mGluR5- VSV- G-H3R-YFP-CFP. Data represents means ± S.E., n = 3. ** significantly different (p<0.01) from the histamine treatment and imetit treatment as determined by one-way ANOVA followed by Dunnett's post test.

Fig. 4

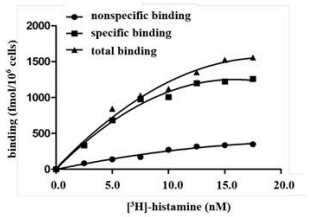

Figure 4. Modifications to generate the H3R intramolecular FRET sensor have similar binding characteristics of the H3 receptor. Saturation [^{3}H]-histamine binding studies were performed on intact Flp-In ^{TM} T-Rex ^{TM} 293 cells induced to express mGluR5-VSV-G-H3R-YFP-CFP. Binding was performed with a range of concentrations of [^{3}H]-histamine (0.4-16 nM) to construct saturation binding curves. Specific binding was defined as the difference between total binding and nonspecific binding observed in the presence of 10 µM clobenpropit. Experiments shown are representative of means ± S.E., *n* = 3.

Fig. 5

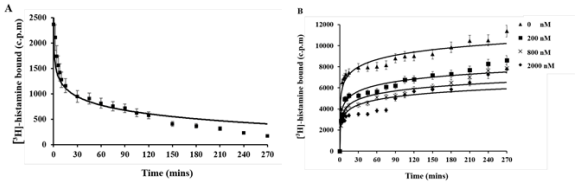

Figure 5. Characterizations of the kinetic parameters of [^{3}H]-histamine. To determine Koff (**A**) Stable cells membranes (10 µg well^{-1}) were preincubated with [^{3}H]-histamine until equilibrium was obtained. Reassociation of [^{3}H]-histamine was then prevented with the addition of 1 µM (final concentration) clobenpropit at the indicated time points. Data was bet fitted using a one-phase exponential decay function to produce a $t_{1/2}$ estimate. This was converted into a Koff value by using Equation 1, as detailed in the Methods. Data represents means ± S.E., *n*=3. The Kon (**B**) was determined by incubation of stable cell membranes (10 µg well^{-1}) with the indicated concentrations of [^{3}H]-histamine for various time points. Data was fitted using a one phase exponential association function to yield an observed on-rate (Kob). The Kon value was calculated using Equation 2, as detailed in the methods. Data represents means ± S.E., *n*=3.

Fig. 6

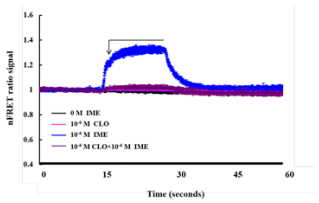

Figure 6. FRET signal increase due to agonist stimulation is abolished by co-addition of H3R antagonist. The H3R intramolecular sensor cells were pre-treated with 1×10^{-6} M clobenpropit (CLO) for 20 min, following which studies were conducted as described in Figure. 3. The H3 receptor antagonist clobenpropit did not modulate the FRET signal of mGluR5-VSV-G-H3R-YFP-CFP when used alone, but when added concurrently with imetit (IME) blocked the effect of the agonist. Data represents means ± S.E., n=5.

Fig. 7

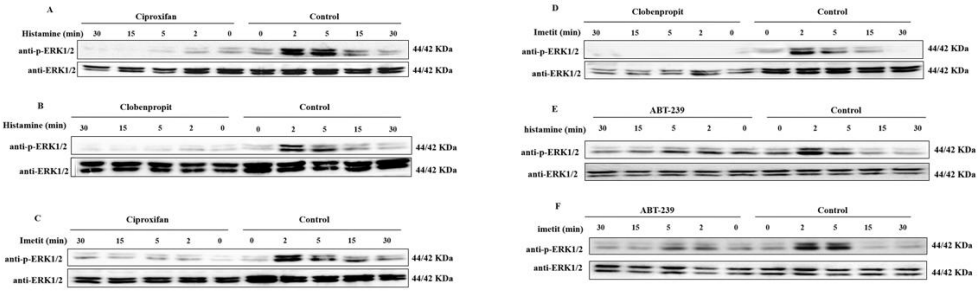

Figure 7. Effect of the H3R antagonists ciproxifan and clobenpropit on the intramolecular sensor mediated ERK1/2 activation. Serum-starved H3R cells were pretreated with 1×10^{-6}M ciproxifan for 1 h. Cells were then stimulated with 1×10^{-6} M histamine (**A**) or imetit (**C**) for the indicated time-periods. Similarly, serum starved H3R cells were pretreated with 1×10^{-6} M clobenpropit for 20 min, and the cells were stimulated with 1×10^{-6} M histamine (**B**) or imetit (**D**) for the indicated time-periods. The expression of phosphorylated ERK (p-ERK) and total ERK were analysed by western blotting. Moreover, serum starved H3R cells were pretreated with 1×10^{-6} M ABT-239 for 20 min, and the cells were stimulated with 1×10^{-6} M histamine (**E**) or imetit (**F**) for the indicated time-periods. The expression of phosphorylated ERK (p-ERK) and total ERK were analysed by western blotting.

Fig. 8

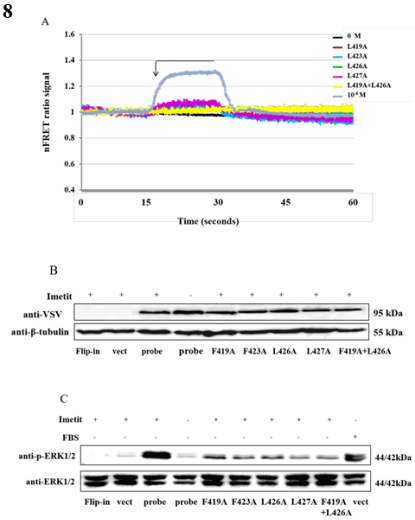

Figure 8. The effect of F419A, F423A, L426A, L427A and F419A+L426A point mutations on the FRET signal and phosphorylation of ERK from H3R sensor treated with agonist. The point mutants F419A, F423A, L426A, L427A and double mutant F419A+L426A were introduced into the mGluR5-VSV-G-H3R-YFP-CFP construct. Flp-In ™ T-Rex ™ 293 cells expressing these variants in response to doxycycline were generated. **A**. 1×10^{-6} M imetit was added at the indicated point, and the FRET signal was detected. **B** and **C**. The expression of the construct VSV-G tag and phosphorylation of ERK were measured by western blotting analysis. Flp-in: Flp-In™ T-REx™ 293 cells; vector: pcDNA5/FRT/To vector; probe: p5-mGluR5- VSV- G-H3R-YFP-CFP